Received: 7 November 2022 | Revised: 4 January 2023 | Accepted: 30 January 2023

DOI: 10.1002/jrs.6506

SPECIAL ISSUE - RESEARCH ARTICLE

Journal of RAMAN SPECTROSCOPY WILEY

Raman study of several Cu-bearing complex minerals from the guano deposit at Pabellón de Pica, Tarapaca region, Chile

Filip Košek[1] | **Ivan Němec**[2] | **Jan Jehlička**[1]

[1]Institute of Geochemistry, Mineralogy, and Mineral Resources, Faculty of Science, Charles University, Prague, Czech Republic

[2]Department of Inorganic Chemistry, Faculty of Science, Charles University, Prague, Czech Republic

Correspondence
Filip Košek, Institute of Geochemistry, Mineralogy, and Mineral Resources, Faculty of Science, Charles University, Albertov 6, 128 00 Prague, Czech Republic.
Email: filip.kosek@natur.cuni.cz

Funding information
Center for Geosphere Dynamics, Grant/Award Number: UNCE/SCI/006

Abstract

Pabellón de Pica, Tarapaca, Chile, is a former guano mine exploited in the late 19th and early 20th centuries. Guano is in a direct contact with Cu sulfide mineralization leading to the formation of minerals with a highly unusual chemical composition, especially Cu-organic complexes and nitrogen-bearing phases. In this work, we report results of the Raman spectroscopic investigation of several unique Cu-bearing minerals that are the result of supergene processes at the Pabellón da Pica site. We focus on several minerals with new and interesting structure types which were described from this locality for the first time, namely, antipinite (K–Na–Cu oxalate), ammineite (Cu ammine complex), chanabayaite (Cu ammine triazolate complex), and joanneumite (Cu isocyanurate). The Raman spectra contain specific bands attributed to the characteristic vibrations of the molecular groups present in the minerals (oxalate, ammine, triazolate, and isocyanurate groups) and vibrations within Cu-centered polyhedra. A comparison was made with the vibrational spectra of related minerals and synthetic phases, which revealed substantial proliferation and shifting of numerous bands, which is in agreement with the complex composition of the investigated minerals. The results obtained appropriately complement known structural and spectroscopic data published previously.

KEYWORDS

ammine, Cu complexes, organic minerals, oxalates, Raman spectroscopy

1 | INTRODUCTION

The northern coast of Chile is known for extensive guano deposits of the seabird origin.[1] The Peruvian–Chilean coastal upwelling system ensured the production of enough food to support large bird colonies, where excreta, carcasses, and eggshells could accumulate.[2–4] In a dry and hot subtropical climate, the material does not suffer from serious decomposition but will instead undergo a transformation to rock-like material during the aging process. Because guano under these conditions still contains a large part of the nitrogenous organic matter and N-rich compounds in general, it is denoted as nitrogenous guano in contrast to phosphatic guano from which most nitrogenous compounds were washed out, leaving only phosphate phases in the material.[1,5,6] There

is evidence that seabird guano was exploited in this region because precolonial cultures as fertilizer.[7,8] The importance of guano for modern agriculture was recognized during the nineteenth century, stimulating prospecting and mining of coastal guano deposits in Peru and Chile.[1] The peak of production was in the late 19th and early 20th centuries. Guano and nitrate material was exported worldwide until the decline after World War I, although most of the deposits were already mined to exhaustion at those times.[9,10]

Aged nitrogenous guano deposits can host an interesting suite of uncommon minerals. In general, N-rich organic compounds such as uric acid are rapidly decomposed by microorganisms, with the most stable products appearing to be oxalates under certain conditions.[11,12] A part of nitrogen is volatilized and released into the atmosphere,[13,14] but some is trapped in the form of ammonium salts or nitrates. The decomposition process can be aerobic or anaerobic but generally requires water income and therefore is very slow in the dry region of the Chilean coast. Therefore, nitrogen is not completely removed from the material and is denoted as a nitrogenous guano.[1,15] Additional elements can be introduced by the sea spray.[1,16] Minerals associated with nitrogenous guano deposits can include oxammite (NH_4 oxalate), whewellite (Ca oxalate), arcanite K_2SO_4, mascagnite $(NH_4)_2SO_4$, sal ammoniac NH_4Cl, halite NaCl, and ammonium and/or Ca phosphates such as struvite $NH_4MgPO_4{\cdot}6H_2O$, as well as urates.[1,5,16,17] However, unique forming conditions occurred at the site of the former mine at Pabellón de Pica, Tarapaca. Here, seabird guano was deposited on the slopes of a headland ~300 m high composed of hornblend gabbro.[1] The rock hosts a small disseminated Cu mineralization (mainly chalcopyrite, $CuFeS_2$) that is in the direct contact with guano.[18] Aggressive compounds originating from guano heavily altered and cracked the base rock.[19] The combination of conditions is exceptional unique, leading to the formation of minerals with a highly unusual chemical composition, especially nitrogen-bearing and organometallic complexes.[18,20–26] The exact forming mechanisms are not well understood, but the involvement of special microbial communities is considered. Although Pabellón de Pica was a former mine, there is no obvious anthropogenic influence on the formation of rare copper minerals.[19] Interestingly, there is no report on this unique mineralogy from the time of the original prospecting of the site in the 19th century (see the references in Hutchinson[1]).

Raman spectroscopy can help with future investigation of the origin of these unusual mineral phases, as it has already proven to be a powerful tool for the identification and characterization of other organic minerals.[27–29] In addition, being relatively simple and generally nondestructive, Raman spectroscopy is an ideal method to study such scarce minerals.[30] Knowing of spectral characteristics is therefore crucial to distinguish between different phases; however, studies of the vibrational spectrum of several minerals remain incomplete. In this work, we report the Raman spectroscopic description of several unique phases that were described from Pabellón de Pica as new minerals, including antipinite (K–Na–Cu oxalate), ammineite (Cu ammine complex), chanabayaite (Cu ammine triazolate complex), and joanneumite (Cu isocyanurate).

2 | MINERAL DESCRIPTION

Antipinite, $KNa_3Cu_2(C_2O_4)_4$, is an anhydrous oxalate with a unique combination of elements, and it is also one of five currently known copper oxalates. Antipinite is not the only Cu oxalate that forms the interaction between guano and copper sulfides, because moolooite $Cu(C_2O_4){\cdot}nH_2O$ is also believed to have the same origin.[31] Antipinite is a triclinic mineral with the *P*-1 space group. The structure (Figure 1) consists of planar oxalate groups (C_2O_4) that interconnect via O atoms a layer of Na atoms and a layer of Cu atoms with pairs of K atoms. The coordination of oxalates leads to the asymmetry of carboxylate groups, which is reflected in two groups of CO bonds lengths—that is, 1.221(2) to 1.232(3) Å and 1.277(2) to 1.288(3) Å. The Cu-centered bipyramidal polyhedra are distorted with apical O atoms forming long Cu^{2+}—O bonds which is typical due to the Jahn–Teller effect. Cu(2) polyhedra share common edges to form a column along the *a* axis, resulting in the layer when combined with a pair of Cu(1) polyhedra. Potassium atoms then occupy the void space in this layer. The other layer is built up of three different Na-centered polyhedra connected via common edges.[20]

Ammineite, $CuCl_2(NH_3)_2$, is the first mineral discovered to incorporate ammine groups (NH_3) into the structure and currently belongs to complex halides.[32] Ammineite is orthorombic, the space group *Cmcm*. The basic structural unit consists of a Cu atom that is coordinated by two NH_3 groups and two Cl atoms, forming a planar *trans*-diammine-dichlorido-copper(II) complex (Figure 2A). This unit is layered parallel to (001) and oriented with Cl(1)—Cu—Cl(2) to [010] and N—Cu—N parallel to [100]. The central Cu atoms are connected to two additional Cl atoms from adjacent complexes by long Cu—Cl bonds. The result is a distorted octahedron with four equatorial bonds to N and Cl atoms and two apical bonds to Cl, described as the typical (4 + 2) configuration for Cu-centered polyhedra. In addition, weak hydrogen

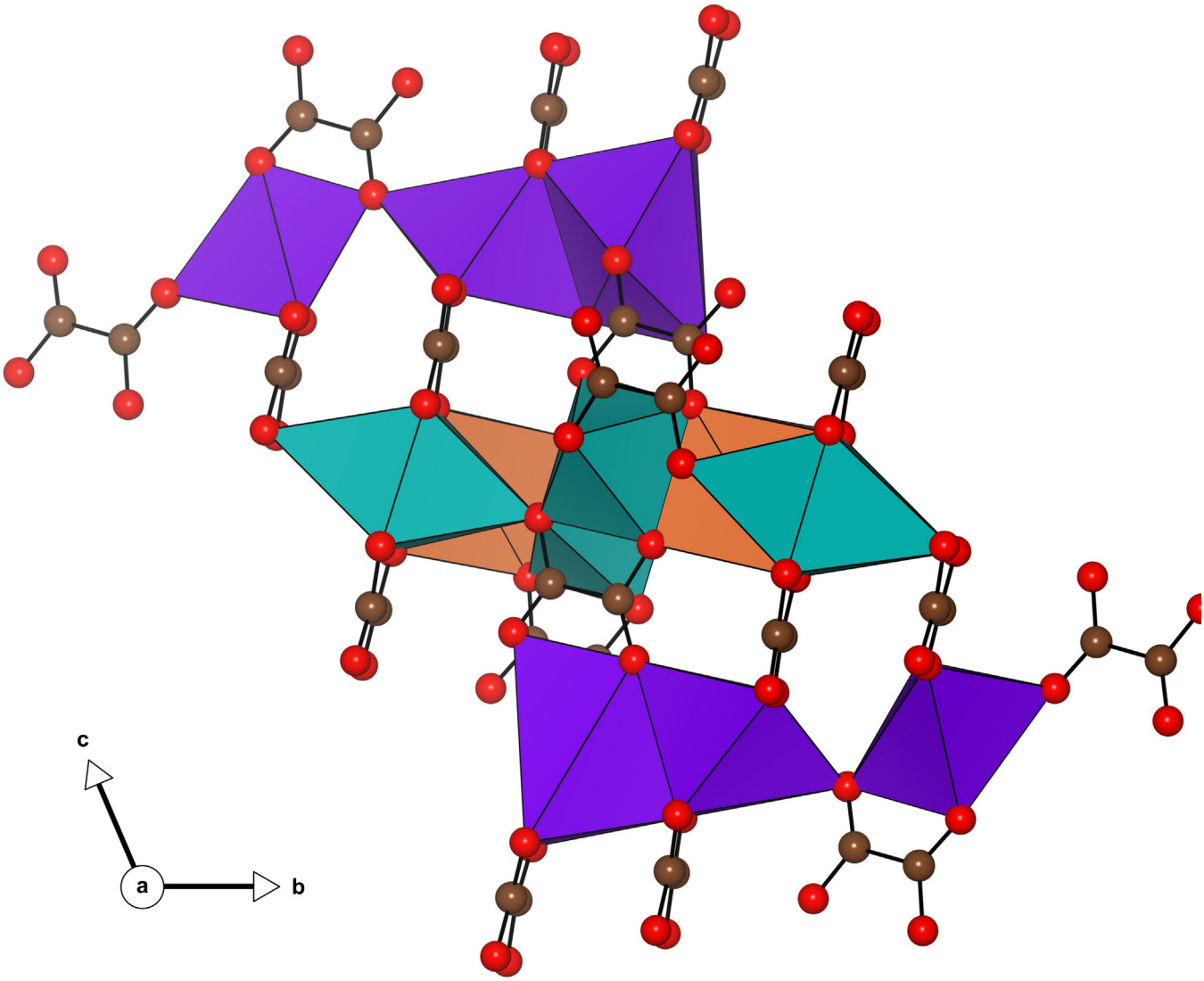

FIGURE 1 Crystal structure of antipinite. The legend for the coordination polyhedra: Cu octahedra—turquoise, Na-centered polyhedra—orange, K-centered polyhedra—purple. After Chukanov et al.[20]

bonds N—H···Cl connect the complexes from one layer to the next and also within the (001) layers.[18]

Chanabayaite, $CuCl(N_3C_2H_2)(NH_3) \cdot 0.25H_2O$ or $Cu_2(N_3C_2H_2)Cl(NH_3,Cl,H_2O,\square)_4$, is an orthorhombic mineral (the space group *Imma*) containing a triazolate group, more specifically 1,2,4-triazolate, which is probably an alteration product from another triazolate phase. The structure (Figure 2B) represents a new structure type, consisting of zig-zag chains of Cu(1) polyhedra along the *b* axis. These polyhedra have four equatorial Cu—N bonds and two longer apical Cu—Cl bonds, with Cl atoms acting as the connection between Cu(1) polyhedra. The other Cu(2) polyhedra are isolated and linked to the chains via triazolate groups. The N(1) atoms of two triazolate anions are apical in the Cu(2) polyhedron, and four equatorial *A* sites are mixed or with incomplete occupancy ($A = (NH_3)_{0.5}(H_2O)_{0.125}(OH)_{0.075}(Cl)_{0.175}$).[22]

Joanneumite, $Cu(C_3N_3O_3H_2)_2(NH_3)_2$, is currently the only known isocyanurate mineral present in nature. It has a triclinic symmetry with the *P*-1 space group. Structurally, the square-planar fundamental building unit consists of a central Cu atom coordinated via Cu—N bonds by four ligands, two ammine groups, and two isocyanurate groups (i.e., tri-oxo tautomer derived from cyanuric acid, $C_3N_3O_3H_2$) (Figure 2C). These units are interconnected via pairs of hydrogen bonds between isocyanurate rings, building a layer parallel to (−122). The three hydrogens of the ammine groups are involved in hydrogen bonds that interconnect these layers up and down to a three-dimensional network.[23]

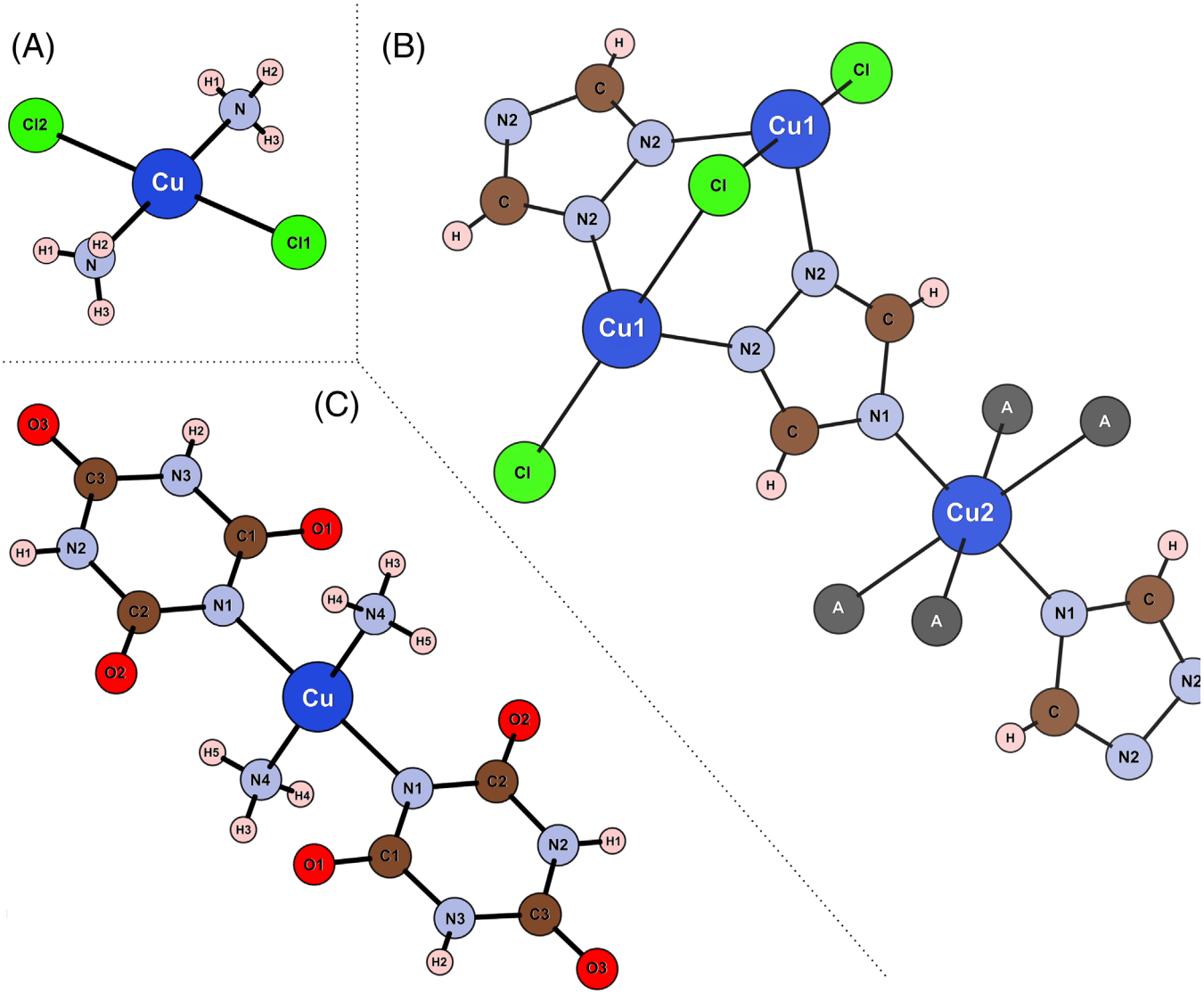

FIGURE 2 The fundamental structural units of (A) ammineite,[18] (B) chanabayaite,[22] and (C) joanneumite.[23]

3 | EXPERIMENTAL

3.1 | Samples

The minerals investigated in this study were provided by Jaroslav Hyršl (Prague, CZ) from his private collection. All samples originate from the type locality of Pabellón de Pica, Tarapaca region, Chile. The individual phases were identified within the host rock by the specific color, crystal shapes, and aggregate appearance (Figure 3). Antipinite is represented by finely grained aggregates of blue to pale blue color, very similar to the specimen described by Chukanov et al. (Figure 3A).[20] Ammineite forms deep blue masses with green atacamite on translucent halite (Figure 3B). Chanabayaite is easily to be recognized as clusters of blue prismatic crystals (Figure 3C). Finally, the microcrystalline aggregates of joanneumite are very characteristic of purple color (Figure 3D). The presence of other phases in the samples, such as aforementioned atacamite, was also verified by Raman spectroscopy.

3.2 | Raman spectroscopy

To obtain Raman spectra, the samples of organic minerals were placed on the stage of a Leica microscope, equipped with 5×, 20×, 50×, 100×, and long focus 50× objective lenses. The microscope is part of a multichannel Renishaw InVia Reflex spectrometer coupled with a thermoelectrically cooled CCD detector, which enabled recording of the signal within the 100–4000 cm^{-1}

spectral wavenumber range and with a spectral resolution of 2 cm^{-1}. Excitation was provided either by a 514.5-nm Ar-ion laser (20 mW at the source) or by a near-infrared diode laser emitting at 785 nm (320 mW at the source). To achieve enhanced signal-to-noise ratios, typically 10 to 20 scans were accumulated, each 20 s exposure time. To avoid any possible phase changes or damage, the lasers operated at 5% to 10% of the

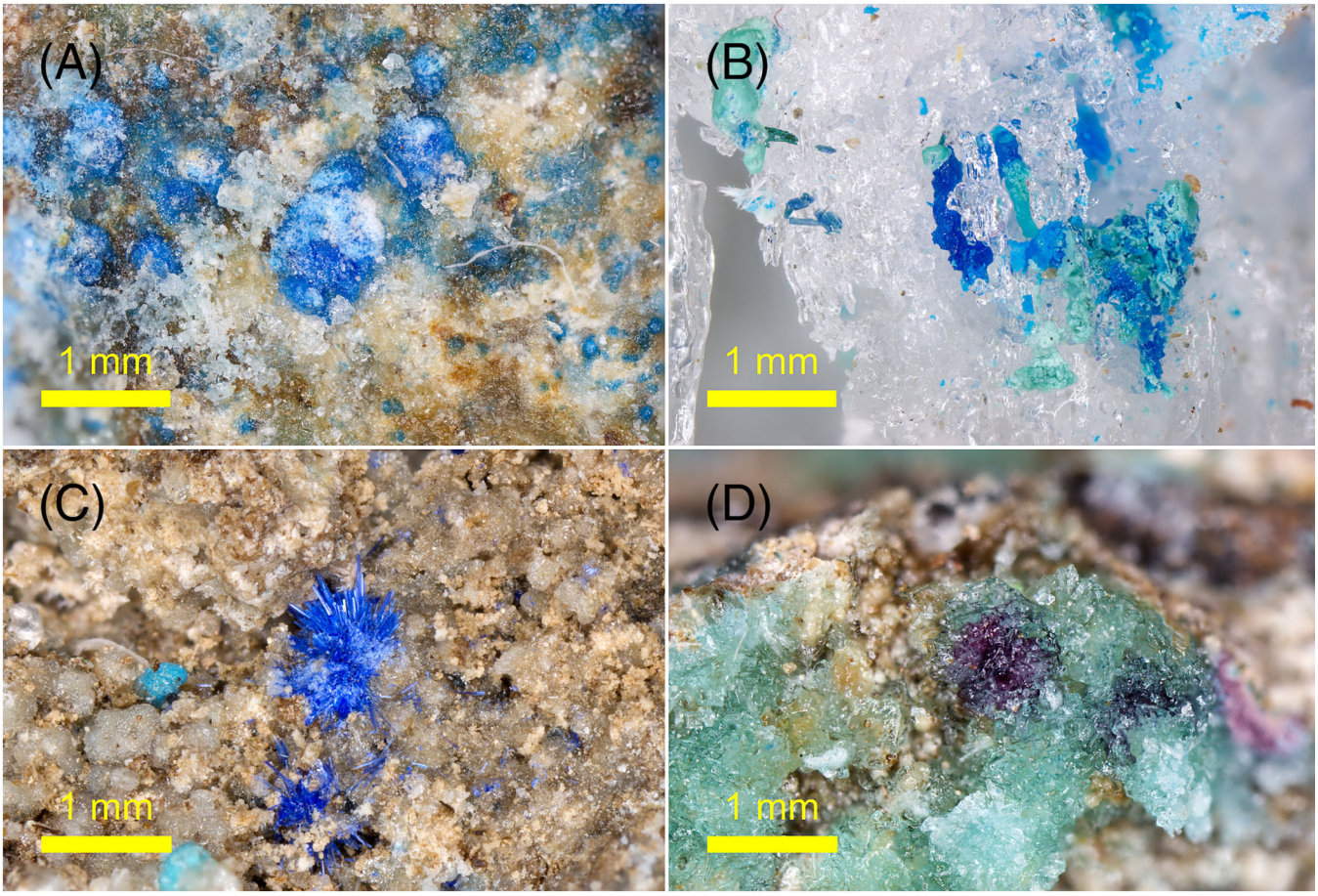

FIGURE 3 Photographs of the investigated minerals—(A) blue antipinite, (B) blue ammineite, (C) blue prismatic chanabayaite, and (D) purple joanneumite.

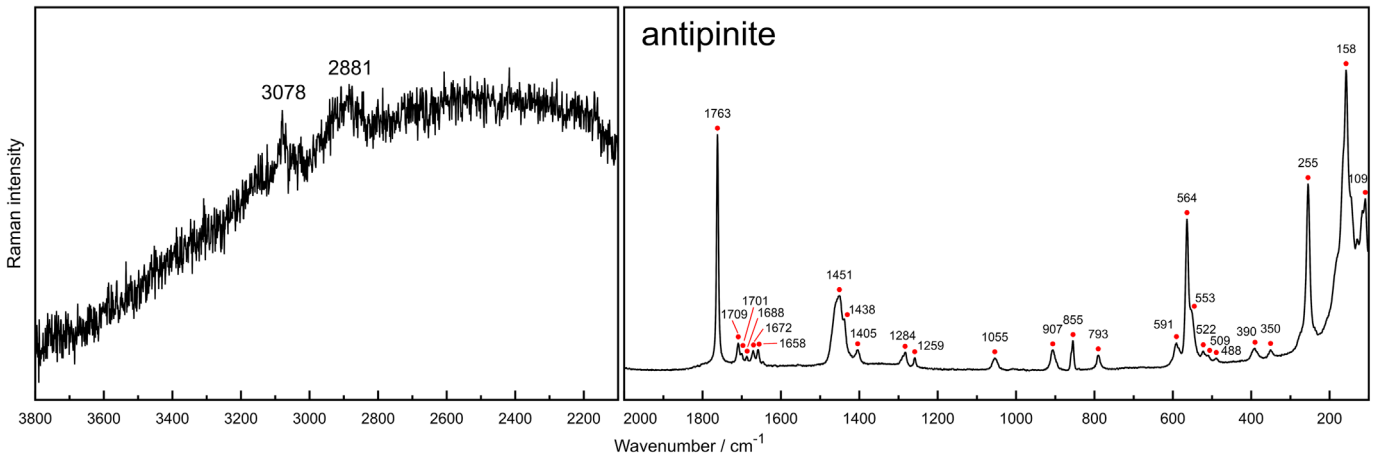

FIGURE 4 Raman spectrum of antipinite in the 100–2000 and 2000–3800 cm^{-1} regions.

maximum output and approximately half of that energy reaches the sample. After each measurement, the samples were visually checked for signs of degradation. Polystyrene standards were used to verify internal calibration. The spectral data were acquired using Wire 2.0 spectral software. Mineral samples were generally measured as they were obtained, without any additional preparation. Spectral analysis and treatment were performed using the GRAMS/AI 9.3 software package. The only advanced technique used was the peak fitting Gaussian–Lorentzian function for the identification of the individual bands in several cases.

4 | RESULTS AND DISCUSSION

4.1 | Antipinite

The Raman spectrum of antipinite (Figure 4) displays a band arrangement and complexity different from most of other oxalate minerals known.[33,34] However, the spectral features of the oxalate group can be distinguished, and a general behavior closely follows the Raman spectrum of another Cu oxalate, wheatleyite $Na_2Cu(C_2O_4)_2{\cdot}2H_2O$.[35,36] The bands of COO antisymmetric stretching vibrations are found in the 1600–1700 cm^{-1} range, with five bands at 1658, 1672, 1688, 1701, and 1709 cm^{-1}. The origin of the band at 1763 cm^{-1} is unclear. A similarly strong band can also be found in the spectrum of antipinite in the RRUFF database (R160005).[37] This very strong band is located at frequencies higher than the carboxylate group for most of other oxalates. In addition, bands of these vibrations are typically weak in Raman spectra. To some extent, similar behavior was also reported, for example, for oxalic acid,[38] and wheatleyite where it is related to the existence of free C═O bonds.[35] However, such free C═O bonds are not present in antipinite.[20] Another possible explanation could also be the appearance of combination (overtone) mode, which was observed in Raman spectra of crystalline alkali oxalates.[39] However, even this explanation is inconsistent with the high intensity of the band under discussion. Yet another explanation could be that antipinite is weathered and underwent partially hydration, which resulted in structural changes and arising the observed bands. The symmetric stretching vibrations of the COO group are identified at 1259, 1284, 1405, 1438, and 1451 cm^{-1}. The proliferation of bands in the region of the COO stretching vibrations is probably related to the fact that several structurally independent oxalate groups with asymmetric COO groups (due to coordination) exist in the antipinite structure. The ν(C—C) stretching modes overlapping with δ(COO) bending modes are observed at 855 and 907 cm^{-1}. Two other bands at 793 and 1055 cm^{-1} are observed in that region. The 793 cm^{-1} band can be assigned to the ω(COO) wagging vibration according to similar band for wheatleyite, but the latter has no counterpart in the spectrum of wheatleyite. For the range between 300 and 600 cm^{-1}, multiple Raman bands are observed at 350, 390, 488, 509, 522, 553, and 564 cm^{-1}. These bands can be assigned to the $\nu(M—O)$ stretching modes (where M = Cu, Na, K) overlapping with ω(COO) wagging vibration. Such complexity is in clear contrast with wheatleyite; however, the antipinite structure includes a number of M—O bonds in several metal-centered polyhedra. Bands observed in the low-frequency region below

TABLE 1 Raman bands and suggested assignments for antipinite.

Antipinite $KNa_3Cu_2(C_2O_4)_4$ (oxalate)	Assignments
109 s	Lattice mode
158 vs	Lattice mode
255 s	Lattice mode
350 w	ρ (COO), ν(M—O)
390 w	ρ (COO), ν(M—O)
488 vw	ω (COO), ν(M—O)
509 vw	ω (COO), ν(M—O)
522 w	ω (COO), ν(M—O)
553 sh	ν(M—O), ω(COO)
564 s	ν(M—O), ω(COO)
591 w	ω (COO), ν(M—O)
793 w	ω (COO)
855 w	ν(C—C), δ(COO)
907 w	ν(C—C), δ(COO)
1055 w	?
1259 w	ν_s(COO)
1284 w	ν_s(COO)
1405 w	ν_s(COO)
1438 sh	ν_s(COO)
1451 m	ν_s(COO)
1658 w	ν_{as}(COO)
1672 w	ν_{as}(COO)
1688 w	ν_{as}(COO)
1701 sh	ν_{as}(COO)
1709 w	ν_{as}(COO)
1763 vs	?
2880 w	?
3080 w	?

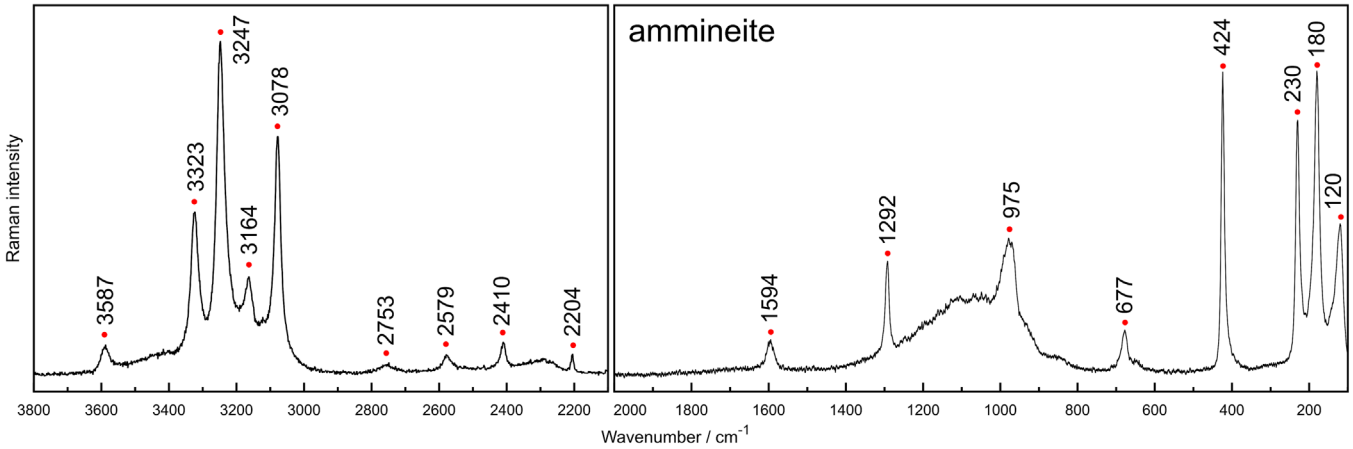

FIGURE 5 Raman spectrum of ammineite in the 100–2000 and 2000–3800 cm^{-1} regions.

300 cm^{-1} can be assigned to lattice modes. We also provide the spectrum recorded within the 2000–3800 cm^{-1} range. No Raman bands associated with antipinite are expected in this area, but we observed two broad bands around 2880 and 3080 cm^{-1}. These could be a possible result of impurities or degradation products in the sample. An overview of the observed bands can be found in Table 1.

4.2 | Ammineite

The Raman spectrum of ammineite (Figure 5) is relatively simple, containing several well-resolved bands. The spectrum also shows good agreement with previously studied IR spectra.[18,40] From a structural point of view, ammineite can be considered as a square-planar $M(NH_3)_2X_2$-type complex; and, therefore, general description and assignments can be derived from the spectroscopic description of halogenoammine complexes.[41–43] The spectrum contains intense signatures associated with the presence of NH_3 groups. Stretching ν(N—H) vibrations of NH_3 ligands can be found at 3323, 3247, 3164, and 3078 cm^{-1}. Other bands in the 2000–4000 cm^{-1} region probably belong to overtones and combination modes. The symmetric $\delta_s(NH_3)$ and antisymmetric $\delta_{as}(NH_3)$ deformation modes are observed at 1292 and 1594 cm^{-1}, respectively. The band of the ρ rocking vibration of NH_3 groups lies at 677 cm^{-1}. The broad band of around 975 cm^{-1} does not have a clear counterpart in the vibrational spectra of ammine complexes and, in addition, was not found in the IR spectrum of ammineite. Therefore, it could be related to an impurity in the investigated sample or the influence of luminescence effects. The other strong signals are assigned to the skeletal vibrations. The strong band at 424 cm^{-1} is assigned to the ν(Cu—N) stretching vibration, while the band at 230 cm^{-1} to the ν(Cu—Cl) stretching vibration. As in the case of other halogenammine complexes,[41] different positions of these skeletal vibrations are expected due to different masses of nitrogen and chlorine atoms, resulting in different force constants of the bonds. The bands recorded at 120 and 180 cm^{-1} are due to either skeletal bending δ(Cu—N—Cu) or lattice

TABLE 2 Raman bands and suggested assignments for ammineite.

Ammineite $[CuCl_2(NH_3)_2]$ (ammine complex)	Assignments
120 s	Lattice mode
180 vs	δ(Cu—N—Cu)
230 vs	ν(Cu—Cl)
424 vs	ν(Cu—N)
677 m	$\rho(NH_3)$
975 m	?
1292 m	$\delta_s(NH_3)$
1594 w	$\delta_{as}(NH_3)$
2204 w	?
2410 w	?
2579 w	?
2753 w	?
3078 s	ν(N—H)
3164 m	ν(N—H)
3247 vs	ν(N—H)
3323 s	ν(N—H)
3587 w	?

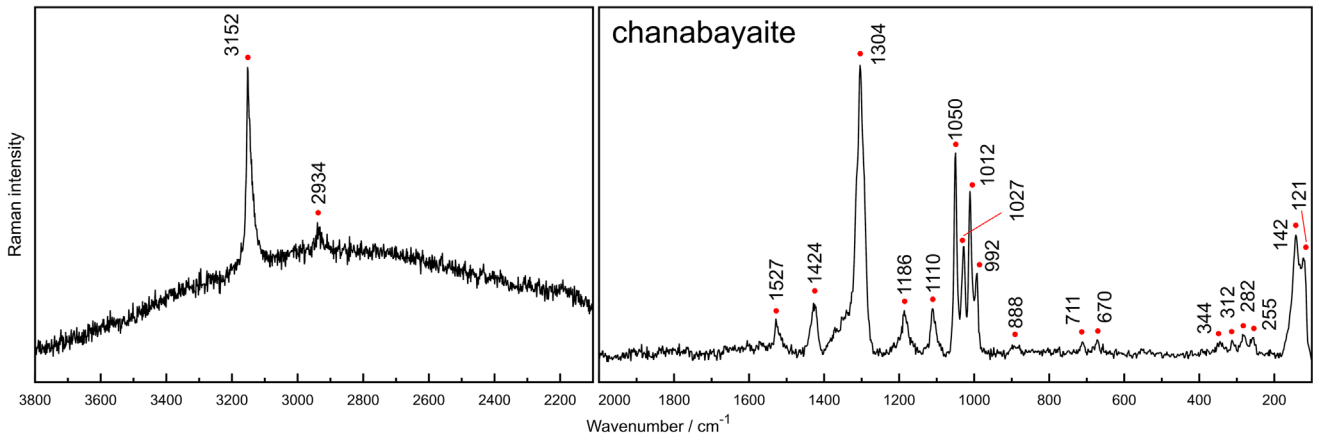

FIGURE 6 Raman spectrum chanabayaite in the 100–2000 and 2000–3800 cm^{-1} regions.

vibrations. Compared with the Raman spectra of other metal ammine complexes,[41–43] such as *trans*-[Pd $(NH_3)_2Cl_2$], the Raman bands in the ammineite spectrum, and especially the bands of skeletal vibrations, are found at lower frequencies. The observed bands can be found in Table 2.

4.3 | Chanabayaite

The Raman spectrum of chanabayaite is shown in Figure 6. The dominant spectral features in the spectrum belong to the vibrations of 1,2,4-triazolate rings.[43] The bands of ν(C—H) stretching vibrations can be observed at 3152 cm^{-1} and numerous intense bands associated with manifestations of the 1,2,4-triazolate ligand can be found in the region ranging from ~1000 to 1550 cm^{-1}, namely, at 1012, 1027, 1050, 1186, 1304, 1424, and 1527 cm^{-1}. These bands are the result of stretching and deformation vibrations of the triazolate rings (formed by N—N and C—N bonds), as well as some of the bands are also associated with in-plane deformation modes of the C—H bonds. The weak band at 888 cm^{-1} and medium intensity band at 992 cm^{-1} can be associated with out-of-plane bending vibrations of the C—H bond, while two other weak bands at 670 and 711 cm^{-1} can be assigned to out-of-plane deformation vibrations of the rings. Although not entirely analogous, because of the more complex crystal structure of chanabayaite, the spectrum shares similarities with the spectrum of sodium 1,2,4-triazolate.[44] In contrast with this salt, however, the bands in the region of stretching vibrations of triazolate rings are systematically shifted to the lower frequencies. Several bands of weak intensity in the low-frequency region (255, 282, 312, and 344 cm^{-1}) can be mainly attributed to the stretching Cu—(N,Cl) vibrations in the Cu-centered octahedra. As mentioned above, the structure of chanabayaite provides special *A* sites of different occupancy on the equatorial plane of the Cu(2)-octahedron, which are partially occupied by the ammine NH_3 ligands and water molecules. The bands of these molecular groups should therefore be observable. However, there is no strong evidence for water-associated bands in the spectrum, and the possible assignment of

TABLE 3 Raman bands and suggested assignments for chanabayaite.

Chanabayaite $CuCl(N_3C_2H_2)(NH_3)\cdot 0.25H_2O$ (triazolate)	**Assignments**
121 s	Lattice mode
142 s	Lattice mode
255 vw	ν(Cu—N,Cl)
282 vw	ν(Cu—N,Cl)
312 vw	ν(Cu—N,Cl)
344 vw	ν(Cu—N,Cl)
670 vw	π(ring)
711 vw	π(ring), $\rho(NH_3)$
888 vw	π(C—H)
992 m	π(C—H)
1012 s	ν(ring), δ(C—H)
1027 s	ν(ring), δ(C—H)
1050 s	ν(ring), δ(C—H), δ(ring)
1186 m	ν(ring), δ(C—H), δ(ring)
1304 vs	ν(ring), δ(C—H)
1424 m	ν(ring), δ(C—H)
1527 m	ν(ring), δ(C—H), $\delta_{as}(NH_3)$
2934 w	ν(N—H)?
3152 s	ν(C—H), ν(N—H)

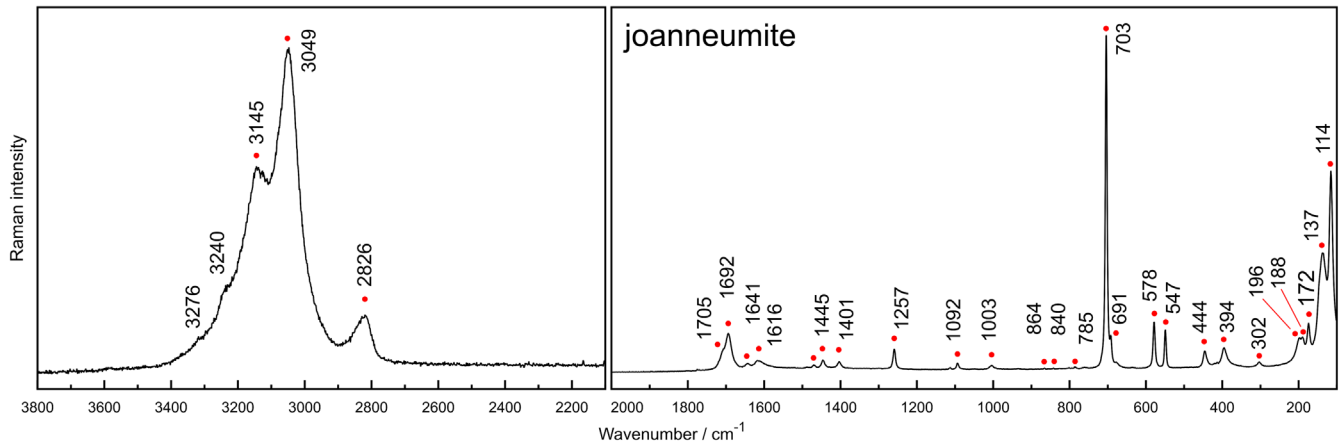

FIGURE 7 Raman spectrum joanneumite in the 100–2000 and 2000–3800 cm^{-1} regions.

TABLE 4 Raman bands and suggested assignments for joanneumite.

Joanneumite $Cu(C_3N_3O_3H_2)_2(NH_3)_2$ (isocyanurate)	Assignments
114 s	Lattice mode
137 s	Lattice mode
172 m	Lattice mode
188 m	Lattice mode, δ(N—Cu—N)
196 m	Lattice mode, δ(N—Cu—N)
302 w	Lattice mode
394 m	δ(N—C═O), ν(Cu—N)
444 m	δ(N—C═O), ν(Cu—N)
547 m	δ(C═O)
578 m	δ(C═O)
691 sh	π(C═O)
703 vs	π(C═O)
785 vw	π(C═O)
840 vw	δ(ring)
864 vw	δ(ring)
1003 w	ν(ring), δ(N—H)
1092 w	ν(ring), δ(N—H)
1111 w	ν(ring), δ(N—H)
1257 m	$\delta_s(NH_3)$, δ(N—H)
1401 w	ν(ring)
1445 w	ν(ring)
1469 w	ν(ring)
1487 vw	ν(ring)
1616 w	ν(ring), δ(N—H), $\delta_{as}(NH_3)$
1641 w	ν(ring), δ(N—H), $\delta_{as}(NH_3)$
1692 m	ν(ring), δ(N—H)

TABLE 4 (Continued)

Joanneumite $Cu(C_3N_3O_3H_2)_2(NH_3)_2$ (isocyanurate)	Assignments
1705 sh	ν(C═O)
2826 m	ν(N—H)
3049 s	ν(N—H)
3145 s	ν(N—H)
3240 sh	ν(N—H)
3276 sh	ν(N—H)

the weak band at 2934 cm^{-1} to water is speculative. Instead, this band can be due to the stretching modes of NH_3 groups. The band at 1527 cm^{-1} can also be related to the antisymmetric bending vibrations of NH_3 ligands. The presence of this ligand could also be associated with the bands at 3152 and 711 cm^{-1}. In that case, these bands would represent stretching ν(N—H) and rocking $\rho(NH_3)$ vibrations. However, the contribution of ammine ligands to the band at 3152 cm^{-1} would be rather small, because this band is prominent for ν(C—H) stretching vibrations. Table 3 summarizes the Raman bands observed for chanabayaite.

4.4 | Joanneumite

Joanneumite shows relatively simple Raman spectrum with a combination of intense and weak Raman bands (Figure 7). As in the case of previous minerals, the observed Raman bands can be assigned to the specific molecular groups or skeletal vibrations. In joanneumite, the dominant structural subunit is the isocyanurate

ligand, which represents tri-oxo tautomer derived of cyanuric acid. The suggested assignment is based on the work of Seifer,[45] Bojar et al.,[23] and Rostkowska et al.[46] Broad bands in the 2800–3400 cm^{-1} region can be assigned to the stretching ν(N—H) vibrations. The weak bands recorded at 1705 and 1774 cm^{-1} are characteristic for the stretching ν(C═O) vibrations of the carbonyl group. The strong band at 703 cm^{-1} and the weak bands at 691 and 785 cm^{-1} are assigned to the out-of-plane π(C═O) deformation vibrations. The manifestation of isocyanurate ring stretching vibrations is present in the region ranging from 1350 to 1700 cm^{-1}. The weak bands located at 1003, 1092, and 1111 cm^{-1} were assigned to mixed ν(ring) and δ(N—H) modes. Deformation vibrations of the ring correspond to the weak bands observed around 840 and 864 cm^{-1}. The bands recorded at 650–800 and 500–600 cm^{-1} regions were assigned to out-of-plane and in-plane deformation vibrations of isocyanurate carbonyl group, respectively. The skeletal stretching ν(Cu—N) vibrations overlapping with deformation δ(N—C═O) modes were attributed to medium intensity bands at 444 and 394 cm^{-1}. A set of bands in the low-frequency region around 114, 137, 172, 188, 196, and 302 cm^{-1} could be assigned to lattice modes. The presence of the ammine ligands in the crystal structure of joanneumite is manifested by the bands of stretching ν(N—H), deformation $\delta_{as}(NH_3)$ and $\delta_s(NH_3)$ modes recorded at 2800–3400 cm^{-1} region, 1641, 1616, and 1257 cm^{-1}, respectively. Lastly, skeletal deformation modes δ(N—Cu—N) are also expected at the 180–200 cm^{-1} region. Overview of Raman bands recorded for joanneumite is given in Table 4.

5 | CONCLUSIONS

A suite of copper and/or nitrogen-bearing complex minerals antipinite, ammineite, chanabayaite, and joanneumite, representing new structural types, has been characterized by Raman spectroscopy. We did not experience severe analytical difficulties to record the Raman spectra, despite the fact that organic minerals can be prone to fluorescence emission and decomposition after exposure to the excitation laser.[29] The spectra were described based on the structural peculiarities of the minerals by comparison with the vibrational spectra of related minerals and synthetic phases. Antipinite, the only oxalate mineral investigated within the study, showed a Raman spectrum different from that of most other known oxalates but showed good agreement with another Cu oxalate, wheatleyite, and the bands of fundamental oxalate vibrations can be distinguished. However, we observed an unusually intense band (1763 cm^{-1}) in the COO antisymmetric stretching region of the oxalate group, although such bands are typically weak in Raman spectra. Although the phenomenon was observed for wheatleyite or oxalic acid, the explanation for these phases cannot be easily applied to antipinite due to structural differences, and therefore, the correct assignment of this band remains elusive. Ammineite, being a copper halogen ammine complex, showed a simple Raman spectrum that resembles spectra of other metal ammine complexes. Consequently, the spectrum was dominated by the vibrations of the NH_3 ligands, as well as the Cu—(N,Cl) vibrations. In contrast to the simplicity of the ammineite spectrum, chanabayaite and joanneumite provided complex Raman spectra due to the organic anions involved in their structures, 1,2,4-triazolate and isocyanurate. However, in both cases, the mineral spectra contain characteristic Raman bands of their synthetic analogs or precursors (1,2,4-triazolate and isocyanuric acid). The proliferation of bands and notable shifts in the band positions observed in the spectra can be explained by the structural arrangements of Cu cations, organic anions, and other ligands, which are more complicated than in the case of isolated triazole and isocyanuric acid molecules.

Generally speaking, each mineral has its own characteristic spectrum, which supports other structural or spectroscopic data reported previously. On this basis, the minerals can be successfully identified unambiguously in natural samples. Because Raman spectroscopy is a non-destructive technique and allows microscopic investigation of mineral aggregates of the complex composition, this method can be successfully used in future investigations at the guano deposits of Pabellón de Pica, Chille, and help to decipher the complicated mineral relations and forming pathway at this site or in other environments where the investigated or similar complex Cu-bearing phases can occur.

ACKNOWLEDGMENTS

This work was supported by Center for Geosphere Dynamics (UNCE/SCI/006). The authors also thank Jaroslav Hyršl for providing rare mineral specimens.

ORCID

Filip Košek https://orcid.org/0000-0002-5675-7913
Ivan Němec https://orcid.org/0000-0001-9630-3169
Jan Jehlička https://orcid.org/0000-0002-4294-876X

REFERENCES

[1] G. E. Hutchinson, *Bull. Am. Mus. Nat. Hist.* **1950**, *96*, 1.
[2] H. Tovar, V. Guillen, M. E. Nakama, in *The Peruvian Anchoveta and Its Upwelling Ecosystem: Three Decades of Change*, (Eds: D. Pauly, I. Tsukayama), ICLARM Studies and Review Vol. 15, Instituto del Mar del Peru, **1987** 208.

[3] H. Weimerskirch, S. Bertrand, J. Silva, C. Bost, S. Peraltilla, *Mar. Ecol. Prog. Ser.* **2012**, *458*, 231.
[4] K. Ludynia, S. Garthe, G. Luna-Jorquera, *J. Ornithol.* **2010**, *151*, 103.
[5] D. J. Cullen, *Sedimentology* **1988**, *35*, 421.
[6] C. Landis, D. Craw, *J. R. Soc. N. Z.* **2003**, *33*, 487.
[7] F. Santana-Sagredo, R. J. Schulting, P. Méndez-Quiros, A. Vidal-Elgueta, M. Uribe, R. Loyola, A. Maturana-Fernández, F. P. Díaz, C. Latorre, V. B. McRostie, C. M. Santoro, V. Mandakovic, C. Harrod, J. Lee-Thorp, *Nat. Plants.* **2021**, *7*, 152.
[8] P. Rodrigues, J. Micael, *Ibis* **2021**, *163*, 283.
[9] D. Hollett, *More Precious Than Gold: The Story of the Peruvian Guano Trade*, Associated University Presses, Cranbury, New Jersey, **2008**.
[10] B. Clark, J. B. Foster, *Int. J. Comp. Sociol.* **2009**, *50*, 311.
[11] W. Franke, G. E. Hahn, *Hoppe-Seyler's Z. Physiol. Chem.* **1955**, *299*, 15.
[12] M. Legrand, F. Ducroz, D. Wagenbach, R. Mulvaney, J. Hall, *J. Geophys. Res. Atmos.* **1998**, *103*, 11043.
[13] H. Mizutani, E. Wada, *Ecology* **1988**, *69*, 340.
[14] H. Lindeboom, *Ecology* **1984**, *65*, 269.
[15] E. Schnug, F. Jacobs, K. Stöven, in *Seabirds*, (Ed: H. Mikkola), IntechOpen, Rijeka **2018** 79.
[16] F. Lucassen, W. Pritzkow, M. Rosner, F. Sepúlveda, P. Vásquez, H. Wilke, S. A. Kasemann, *PLoS ONE* **2017**, *12*, e0179440.
[17] H. Winchell, R. J. Benoit, *Am. Mineral.* **1951**, *36*, 590.
[18] H.-P. Bojar, F. Walter, J. Baumgartner, G. Färber, *Can. Mineral.* **2010**, *48*, 1359.
[19] Pabellón de Pica. Chanabaya, Iquique Province, Tarapacá, Chile from Mindat.org https://www.mindat.org/loc-192704.html. Accessed on 4.11.2022.
[20] N. V. Chukanov, S. M. Aksenov, R. K. Rastsvetaeva, K. A. Lyssenko, D. I. Belakovskiy, G. Färber, G. Möhn, K. V. Van, *Mineralog. Mag.* **2015**, *79*, 1111.
[21] N. V. Chukanov, S. N. Britvin, G. Mohn, I. V. Pekov, N. V. Zubkova, F. Nestola, A. V. Kasatkin, M. Dini, *Mineralog. Mag.* **2015**, *79*, 613.
[22] N. Chukanov, N. Zubkova, G. Möhn, I. Pekov, D. Y. Pushcharovsky, A. Zadov, *Geol. Ore Depos.* **2015**, *57*, 712.
[23] H.-P. Bojar, F. Walter, J. Baumgartner, *Mineralog. Mag.* **2017**, *81*, 155.
[24] N. V. Chukanov, G. Mohn, I. V. Pekov, N. V. Zubkova, D. A. Ksenofontov, D. I. Belakovskiy, S. A. Vozchikova, S. N. Britvin, J. Desor, *Mineralog. Mag.* **2020**, *84*, 705.
[25] N. V. Chukanov, G. Mohn, N. V. Zubkova, D. A. Ksenofontov, I. V. Pekov, A. A. Agakhanov, S. N. Britvin, J. Desor, *Mineralog. Mag.* **2020**, *84*, 921.
[26] N. V. Chukanov, N. V. Zubkova, G. Mohn, I. V. Pekov, D. I. Belakovskiy, K. V. Van, S. N. Britvin, D. Y. Pushcharovsky, *Mineralog. Mag.* **2018**, *82*, 1007.
[27] J. Jehlička, H. Edwards, *Org. Geochem.* **2008**, *39*, 371.
[28] J. Jehlička, P. Vitek, H. Edwards, M. Hargreaves, T. Čapoun, *J. Raman Spectrosc.* **2009**, *40*, 1645.
[29] F. Košek, A. Culka, A. Rousaki, P. Vandenabeele, J. Jehlička, *Spectrochim. Acta A* **2020**, *243*, 118818.
[30] L. Nasdala, D. C. Smith, R. Kaindl, M. A. Ziemann, in *Spectroscopic Methods in Mineralogy*, (Eds: A. Beran, E. Libowitzky), Vol. 6, EMU Notes in Mineralogy, Eötvös University Press, Budapest, Hungary, **2004**, Vol. 6 281.
[31] R. Clarke, I. Williams, *Mineralog. Mag.* **1986**, *50*, 295.
[32] J. A. Ferraiolo. Minerals arranged by the Nickel-Strunz (Ver10) Classification System. Available online: https://www.webmineral.com/strunz.shtml. Accessed on 19 December 2022.
[33] R. L. Frost, *Anal. Chim. Acta* **2004**, *517*, 207.
[34] R. L. Frost, M. L. Weier, *J. Raman Spectrosc.* **2003**, *34*, 776.
[35] D. Palacios, A. Wladimirsky, M. C. D'Antonio, A. C. González-Baró, E. J. Baran, *Spectrochim. Acta A* **2011**, *79*, 1145.
[36] R. L. Frost, A. Locke, W. N. Martens, *J. Raman Spectrosc.* **2008**, *39*, 901.
[37] B. Lafuente, R. T. Downs, H. Yang, N. Stone, in *Highlights in Mineralogical Crystallography*, (Eds: T. Armbruster, R. M. Danisi), W. De Gruyter, Berlin **2015** 1.
[38] J. De Villepin, A. Novak, D. Bougeard, *Chem. Phys.* **1982**, *73*, 291.
[39] R. E. Dinnebier, S. Vensky, M. Panthöfer, M. Jansen, *Inorg. Chem.* **2003**, *42*, 1499.
[40] G. M. Barrow, R. H. Krueger, F. Basolo, *J. Inorg. Nucl. Chem.* **1956**, *2*, 340.
[41] P. Hendra, *Spectrochim. Acta A* **1967**, *23*, 1275.
[42] I. Degen, A. Rowlands, *Spectrochim. Acta A* **1991**, *47*, 1263.
[43] K. Nakamoto, *Infrared and Raman Spectra of Inorganic and Coordination Compounds, Part B: Applications in Coordination, Organometallic, and Bioinorganic Chemistry*, John Wiley & Sons, Hoboken, New Jersey **2009**.
[44] F. Billes, H. Endrédi, G. Keresztury, *J. Mol. Struct. THEOCHEM* **2000**, *530*, 183.
[45] G. Seifer, *Russ. J. Coord. Chem.* **2002**, *28*, 301.
[46] H. Rostkowska, L. Lapinski, M. J. Nowak, *Vib. Spectrosc.* **2009**, *49*, 43.

How to cite this article: F. Košek, I. Němec, J. Jehlička, *J Raman Spectrosc* **2023**, *54*(11), 1172. https://doi.org/10.1002/jrs.6506